Reanalyses for dense shelf water cascading in the Cap de Creus Canyon and the atmospheric winter conditions

Author: Helena Fos Serdà
Supervisor: Jesús Peña Izquierdo, jesus.pena@lobelia.earth (1)
University supervisor: Ileana Bladé Mendoza, ileanablade@ub.edu (2)
(1) Lobelia. Parc tecnològic de Barcelona, 8-14 Marie Curie Street, 08042 Barcelona, Spain.
(2) Facultat de Física, Universitat de Barcelona, Martí i Franquès 1, 08028 Barcelona, Spain.*

Abstract: In the Gulf of Lion (GoL), during cold winters, the local northerly winds cool the continental shelf water, increasing its density until it loses enough buoyancy to sink mainly through the submarine canyon of Cap de Creus. This process is known as shelf water cascading. To assess the interannual variability of the intensity of these events in the past decades, we use the reanalysis dataset Med MFC from the Mediterranean Sea, which has proved to correlate well with in-situ observations of cascading. This also provides a 3D view of the water properties and how they evolve in time. Then, we calculate the sea surface heat and buoyancy fluxes that modify the density of the shelf water using the atmospheric ERA5 and hydrological GloFAS reanalyses. The river freshwater input, the heat loss and the precipitation have been proved to influence the density of shelf water and the intensity of cascading. These fluxes are correlated with the modes of climate variability of the Atlantic Ridge (AR) and Scandinavian Blocking (SCAN): positive phases of AR together with negative phases of SCAN in winter create a larger buoyancy loss on the shelf water in the GoL, and vice versa.

I. INTRODUCTION

The area of the Gulf of Lion (GoL), in the north-western Mediterranean, is one of the few areas in the world where surface marine waters can sink to more than 2000 meters thus ventilating the deep oceans with oxygen. The sinking occurs in cold winters, when the northerly wind, locally called Tramuntana, cools the surface of the sea, via two independent phenomena: open-ocean convection and dense shelf water cascading, see figure 1. Open-ocean convection occurs in the dark-blue shaded area in figure 1, and creates Western Mediterranean Deep Water (WMDW), as vertical mixing of all the present water masses in the water column: Atlantic Water (AW), Winter Intermediate Water (WIW), Levantine Intermediate Water (LIW) and old Western Mediterranean Deep Water (WMDW). AW is a water mass from the Atlantic Ocean that enters through the Strait of Gibraltar and is modified as it travels through the Mediterranean Sea. Since its salinity is lower than those formed in the Mediterranean, it is more buoyant and lays above the others. WIW forms in winter in the Northwestern Mediterranean, on the continental shelf, (Juza et al 2013) and is advected offshore. It is very cold (<13°C) and relatively fresh mainly due to the Rhône River discharge and continental runoff (Juza et al 2013). LIW forms in the Levantine Sea in the Eastern Mediterranean (Malanotte-Rizzoli et al 2003) and is advected to the GoL. It is the saltiest water mass, but its relatively warm temperature leads to intermediate densities. The WMDW is the densest water mass with temperatures below 13ºC and is uniquely formed at the GoL. The properties of AW show a wide seasonal cycle because of its interaction with the atmosphere, while those of LIW and WMDW remain constant throughout the year. The characteristics of WIW depend on the conditions of each winter, with a strong interannual variability in its properties and its mass (Juza et al 2013).

Dense shelf water cascading

In winter, Tramuntana winds cool the water of the continental shelf (coloured in light blue in figure 1), by shelf convection: the water on the surface loses heat to the atmosphere and thus loses buoyancy and sinks, mixing the water column vertically from the top to the bottom.

Since the continental shelf is less deep than the basin in the open ocean, the cooling of the shelf water by vertical mixing is quicker and more effective, shelf water can reach temperatures of less than 10ºC (Durrieu De Madron et al 2013)

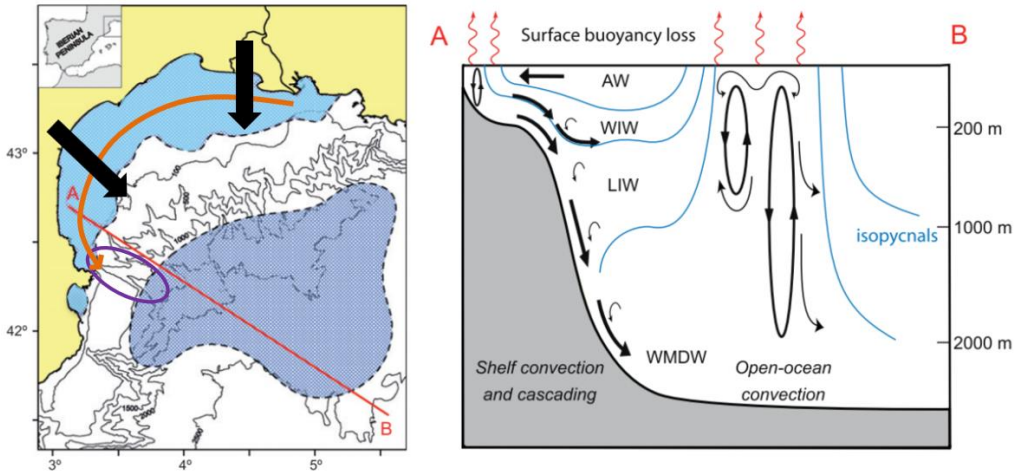

Fig 1. ***Cascading and open-ocean convection.*** Modified form Puig et al. 2013. Left: map of Gulf of Lion. Black arrows are the main wind vectors (Tramuntana), the orange curved arrow is the main path of the dense shelf water, the Cap de Creus canyon is circled by a purple line. Right: cross section showing the dynamics of shelf water cascading and open-ocean convection.

* Electronic address: hfosserd8@alumnes.ub.edu

whereas WMDW remains ca. 12.9ºC (Houpert 2016). Tramuntana wind moves shallow water westward (orange arrow on figure 1 (left), since water is deviated to the right from the wind direction by Coriolis and friction forces, which is known as Ekman transport. During very cold winters, with many days of Tramuntana, the water on the shelf is forced to move cyclonically (Herrmann et al 2008), near the shore, where the low depth implies a shorter water column to cool. Therefore, the shelf water loses temperature, gains density, and loses buoyancy as it travels westward. The presence of Cap de Creus deviates this water southeastward, where the extremely high density of the water makes it less buoyant and forces it to sink through the Cap de Creus Canyon (CCC): shelf water is canalized and flows along the canyon at very high velocities (>80 cm/s), eroding the seafloor, transporting sediment and organic matter from the shelf to the sea bottom (Canals et al 2006). This phenomenon, known as cascading, also occurs in the rest of the canyons of the GoL, although in the CCC is where the densest water is mainly funnelled (Herrmann et al 2008). The method to detect this phenomenon is by noticing an increase in the current velocity along the canyon, simultaneously with a sudden decrease in temperature and salinity (shelf water characteristics). Cascading events have been registered by moorings, which are seafloor-based measurements of seawater properties such as temperature and current velocity, at 500 and 1000 m deep at Lacaze-Duthiers Canyon (LDC) and at 1000 m at CCC (appendix fig A.1). In winters of 2005 and 2012, the cascading shelf water reached more than 2000 m deep and was denser than WMDW (Houpert et al 2016). Unlike open-ocean convection, which can last for a whole winter (Houpert et al 2016**),** intense cascading lasts for one month at most (Canals et al 2006), normally at the end of winter when the shelf water has already cooled enough. Despite the short duration, shelf water cascading is very relevant since it transports organic matter which the deep marine ecosystems depend on (Company et al 2008).

Considering that shelf water gains density by surface heat loss due to Tramuntana winds, and that at the same time, these winds and cooling are responsible for open-ocean convection, the winters with a stronger convection should coincide with the winters with a stronger cascading (Durrieu De Madron et al 2013). However, this is not always the case, for example, in 2010, a very intense open-ocean convection was observed (Houpert et al 2010**)**, whereas the mooring at 1000m deep in the submarine canyons of CCC and LDC did not register any shelf water cascading. Therefore, we may ask: what are the forcing agents for dense shelf water cascading? What causes the interannual variability in its intensity?

Several authors (Hermann et al 2008, Grignon et al 2010, Lebeaupin et al 2017, Margirier et al 2017 and Testor et al 2018) have studied the preconditioning and atmospheric forcing that trigger open-ocean convection in GoL, but the physics behind dense shelf water cascading in CCC have been less studied (Bethoux et al 2002, Bergamasco et al 2010, Ribó et al 2011). While these previous studies of open-ocean convection and/or shelf water cascading are focused on a single winter or ten years at most, little is known about the interannual variability of the past decades. A longer time period, about 30 years long, would allow us to understand the conditions of each winter climatologically. Also, the role of the Rhône River on the modification of the density of the shelf water and its impact on cascading remains unknown. This brings us to use reanalysis datasets in our study: a reanalysis is an optimal estimate of a part of the climate system (oceanic, atmospheric, or hydrological) generated by a numerical model and the assimilation of available observational records. Despite the availability of in-situ measurements at different locations in the GoL, as well as meteorological and oceanic data from l'Estartit reported by the meteorologist Josep Pascual, reanalyses supply continuous data in time and in the three-dimensional space, both oceanic and atmospheric, which permits the better appreciation of cascading and convection processes.

The aim of this study is thus, the use of reanalysis datasets to:

1. Determine the characteristics of water flowing down the CCC and relate them with the intensity of cascading, for a 30-year-long time series.

2. Study the interaction with the atmosphere and the river runoff as a forcing that causes the buoyancy loss of the shelf water in winter.

3. Relate the air-sea fluxes in winter to the main modes of climate variability.

II. DATA FROM REANALYSES

Data from reanalyses have been provided by Copernicus Marine and Copernicus Climate Change Services.

Data from the ERA5 reanalysis (Hersbach et al 2023) have been used for all the atmospheric variables, including wind speed at 10 meters above the surface, daily accumulated precipitation, air temperature at 2 m above the surface, relative humidity, short-wave and long-wave radiation, and geopotential at 500 hPa. This global reanalysis provides hourly averaged data since 1940, with 1/4º latitude-longitude grid width, which corresponds to about a data point every 25 km in the GoL.

To quantify the Rhône River flow to the GoL, we have picked the data point at 43.35ºN and 4.75ºE from GloFAS (Grimaldi et al 2022), which is a global hydrological reanalysis providing daily river discharges with a 1/10º latitude-longitude grid width (~10 km).

Data from the Med MFC reanalysis (Escudier et al 2020) have been used for all the marine variables, including potential temperature, salinity, and current velocity at all depths. This reanalysis of the Mediterranean Sea provides daily averaged data since 1987, with 1/24º latitude-longitude grid width, which corresponds to about a data point every 4 km in the GoL. (See figure A.2 in the appendix for the selection of this dataset).

Given the different resolutions of ERA5 and Med MFC, we must average ERA5 daily and interpolate in space to obtain the same grid width as in Med MFC. The analyses have been extended just until December 2018 because of the availability of the humidity data.

Validation Med MFC with observational data

Since we are specifically interested in dense shelf water cascading the CCC, we have compared the reanalysis data with

the observations of the mooring at CCC, at 1000 m (figure 2). Med MFC is appropriate for our study as it shows the potential temperature (θ) and velocity anomalies concurrent with the observational data from CCC (figure 2), mostly the 2012 and 2013 ones, that correspond to deep cascading events. From 2014 to 2017 and 2020, both the model and the mooring do not detect any anomalies. In 2018 and 2019 a difference is noticed between the simulations and the observations: in 2018, the model detects a single cascading event whereas the mooring detected two short ones, and in 2019 the model does not simulate any. According to the mooring data, these where short cascading events that lasted one or two days and this could be why these are worse reproduced by the model.

The velocity simulated by the model is lower because of the lower spatial resolution of the model, which represents the submarine canyon as a squared channel rather than a steep V-shaped channel where dense water is more localized and gains more acceleration. However, our goal is to view the date of these anomalies, rather than the real value, and this is properly achieved, according to figure 2.

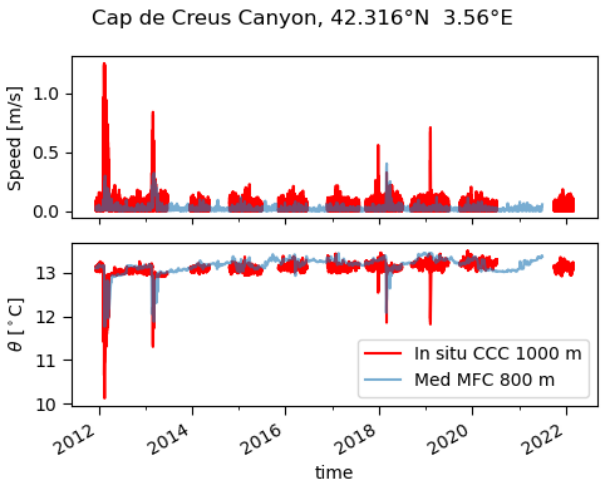

Fig 2. *Comparison of in-situ observations and Med MFC.* These observations correspond to the mooring at CCC seafloor at 1000 m deep, the model output corresponds to that same location, but the depth represented by the model is shallower.

III. METHODOLOGY

Our methods follow the studies of open-ocean convection performed by Somot et al. (2018), who analysed the depth, extension, and persistence of convection for each of their selected winters. Then they related that with the net heat flux and buoyancy loss of each winter, and inferred the associated atmospheric patterns according to their correlations with the net heat flux. Unlike the studies of open-ocean convection, where the interest is in the whole area of the GoL, off-shore, and the river influence is ignored, we will analyse specifically the continental shelf and slope of the GoL, figure 3, and we consider the effect of the Rhône River on the modification of the shelf water properties.

To determine the interannual variability of cascading events and appreciate each of these events, we focus on the water by the seafloor at the shelf and at the CCC. Four locations at CCC have been selected, together with a fifth

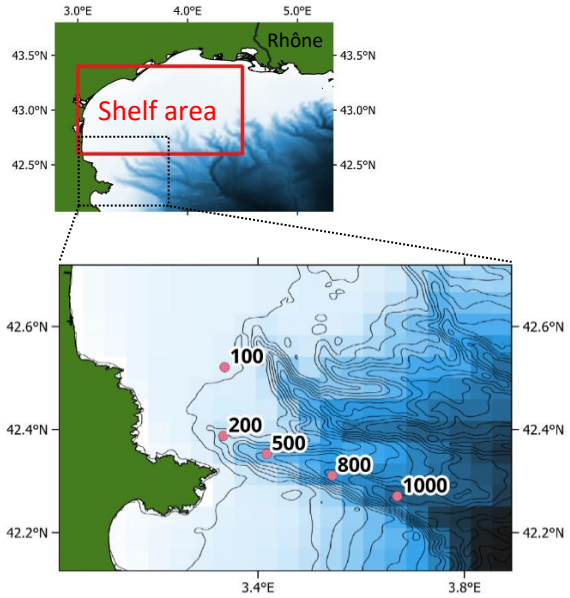

Fig 3. *Selected area and locations.* Top: the red rectangle is the area of the shelf where the ocean-atmosphere fluxes have been calculated (from 42.6 to 43.4ºN and from 3 to 4.5ºE). Notice the Rhône River (black line). Blue shade is the actual bathymetry. Bottom: Selected locations at the bottom of the shelf (100 m) and the Cap de Creus Canyon (200 m, 500 m, 800 m, and 1000 m). Black contours are isobaths every 100 m. The blue pixels correspond to the bathymetry represented by the model.

location over the continental shelf near CCC (see figure 3) at different bottom depths. At each location, we have analysed the properties of seawater in winter: temperature, salinity, and density. These are conservative properties of seawater, which remain unaltered unless the water mixes with other water masses, and reveal the conditions in which the water mass was formed. By doing this, we can identify the water masses at each location at the bottom of CCC, see the differences in temperature, salinity, and density across different winters and, together with the velocity of the current, appreciate the depth at which shelf water cascading has reached. The density of seawater depends on temperature, salinity, and pressure. Since we need to use conservative properties, not conditioned by pressure (and depth), potential temperature (θ) is used. Density (ρ) has been calculated at the same reference pressure, which is the atmospheric pressure, by using the Python package "seawater.eos80" (Bryden 1973, Fofonoff and Millard 1983). Frequently, density is expressed as sigma-theta (σ_θ):

$$\sigma_\theta = \rho(\theta, S) - 1000$$

where ρ is density in kg/m^3, θ is potential temperature in ºC, and S is salinity in PSU.

To evaluate the interaction between the atmosphere and the sea surface, we calculate the heat fluxes. Latent heat flux (Qlatent) and sensible heat flux (Qsensible) are calculated (as in Josey and Schroeder 2023) via the equations:

$$\text{Qlatent} = \rho_a L C_e u (q_s - q_a)$$

$$\text{Qsensible} = \rho_a c_{pa} C_h u (T_s - T_a)$$

Note: the definitions and values of these variables are in Tables A.I and A.II in the appendix.

Notice the Qlatent depends on the wind speed, the dryness of the air and the sea surface temperature (SST). Qsensible depends on the wind speed and the difference in temperature between the air and the sea surface.

Net heat flux (NHF) is the sum of all the turbulent (Qlatent and Qsensible) and radiative (Qshortwave and Qlongwave) fluxes, all expressed in W/m^2:

NHF = Qlatent + Qsensible + Qshortwave + Qlongwave

The sum of Qshorwave and Qlongwave gives the net radiation, which is close to 0 in winter in this area, because Qshorwave and Qlongwave have similar values but opposite signs. Therefore, NHF in winter in GoL mostly depends on the Qlatent and Qsensible fluxes.

Seawater buoyancy loss by heat and mass exchange with the atmosphere, and the river freshwater input, is given by the following formula:

$$B = \underbrace{g\frac{\alpha_\theta \cdot NHF}{\rho_s \cdot c_{ps}}}_{\text{Bt}} + \overbrace{\underbrace{g \cdot \beta \cdot SSS \cdot (P - E + R)}_{\text{Bs}}}^{\text{Bsp}}$$

Where B is the buoyancy flux between the atmosphere and the sea. B < 0 means the sea surface loses buoyancy because it gains density by interaction with the atmosphere. Bt is the buoyancy flux due to thermal variations, Bs is the buoyancy flux due to salinity variations, which depends on the precipitation (P) – evaporation (E) + river input (R). Bsp is the same as Bs but does not include the river influence, just the balance between precipitation and evaporation.

For the definition, values and units of each parameter see the Tables A.I and A.II in the appendix.

The modes of climate variability have been determined following the method used by NOAA CPC (https://www.cpc.ncep.noaa.gov/data/teledoc/telepatcalc.shtml), with the geopotential data (Φ) at 500 hPa, from ERA5, with a spatial coverage from 30°N to 89ºN and from -70°E to 40°E. The geopotential height (Z) is the geopotential divided by the standard gravity (g_0):

$$\mathrm{Z} = \frac{\Phi}{\mathrm{g_0}}, \quad \mathrm{g_0} = 9.81\ \mathrm{m/s^2}$$

Then, the monthly standardized anomalies of Z (Zstand) have been calculated by computing the monthly averaged values of Z, subtracting the climatology values (c) as the mean between 1987 and 2018, and dividing by the standard deviation (SD) for that month:

$$Z\mathrm{stand}_i = \frac{\mathrm{Z}_i - \mathrm{c}_i}{\mathrm{SD}(\mathrm{Z}_i)}$$

i = winter month (December, January, February, and March)

With these standardized anomalies, we have performed a Principal Component Analysis (PCA) or Empirical Orthogonal Function (EOF) analysis using the Python Package "eof" (Dawson 2016) and extracted the three first modes. This yields the three leading EOF, which are dominant geographic patterns of Z anomalies, in the latitude-longitude space, and these are orthogonal (not correlated). The PC time-series of each EOF indicates how the amplitude of each EOF varies in time. The main modes of climate variability are the leading EOF, expressed as the covariance between the leading PC time series and the standardized anomalies of Z. This explains a fraction of the atmospheric variability at 500hPa (about 5500 m high), which has also been quantified for each EOF using the same package of Python. Then, we analyse the Pearson correlation coefficient between each of the three PCs (one for each mode) and the time series of each of the buoyancy fluxes (Bsp, Bs, Bt, B). The aim of this is to evaluate if these interannual variations in air-sea fluxes are due to climate variability, and which modes are more prone to influence each component of the buoyancy fluxes.

IV. RESULTS AND DISCUSSION

In this section, we present the results and discussion from the observed characteristics of the shelf water flowing through the CCC and relate it with the intensity of cascading. Then, we analyse the interaction of the atmosphere and river to explain the interannual variability of this shelf water characteristics, and correlate this with the atmospheric modes of variability.

IV-1. Dense shelf water cascading through CCC

We have represented, for each year, between 1 January and 31 March, the values of potential temperature and salinity at each depth in a T-S diagram. In figure 4, twelve of these diagrams are shown, these are referent winters. Shelf water, at 100 m deep, begins being warm and cools down as winter progresses. The maximum density reached in a wintertime determines the depth at which the water sinks through the CCC via cascading.

The similarities and differences between the T-S diagrams permit the distinction of three possible levels or intensities of cascading.

0. No cascading. The shelf water sinking reaches less than 500 m inside the submarine canyon, because the density of the shelf water does not increase enough, the temperature is relatively warm during the whole winter, AW. Hence, very little WIW is formed.
1. Shallow cascading. The shelf water cools while its salinity decreases, which implies the density of shelf water does not reach the density of the intermediate water at the CCC, composed by LIW. Consequently, the shelf water descends through the CCC up to 500 – 800 m approximately, just above LIW, forming WIW that pushes the LIW down.
2. Deep cascading. The shelf water loses a lot of temperature and remains very salty (>38 PSU), thus it gains extremely large values of density. It exceeds the density of intermediate and deep waters at 500, 800 and 1000 m, composed by LIW and WMDW. Consequently, the shelf water descends through the CCC up to more than 1000 m. The water mass generated by this process is considered a variety of WMDW, which is denser than the usual WMDW formed by open-ocean convection.

Another method to detect cascading events is by observing the cold shelf water flow: representing a time series of the temperature and velocity at one or more locations at the bottom of the canyon, as we have previously shown in figure 2. The complete time series with the model data at two locations of

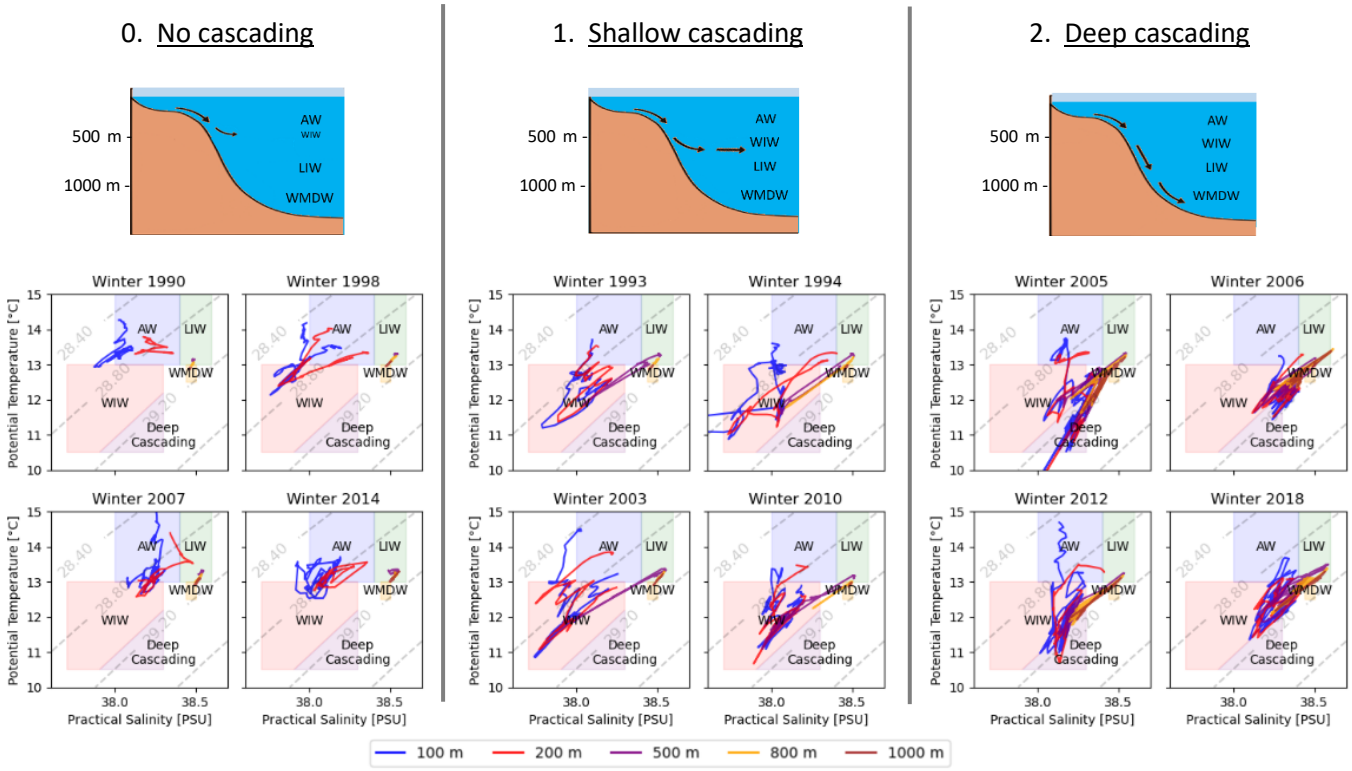

Fig 4. *Cascading illustrations and the associated T-S diagrams from the Cap de Creus Canyon in winter (JFM).* The colour lines show the temporal evolution of the potential temperature and salinity from Med MFC at 100, 200, 500, 800 and 1000 meter of bottom depth along CCC. The colour-shaded polygons represent the corresponding water masses according to the temperature and salinity, following the criterion used by Juza et al 2013. Dashed grey lines represent the density in σ_θ.

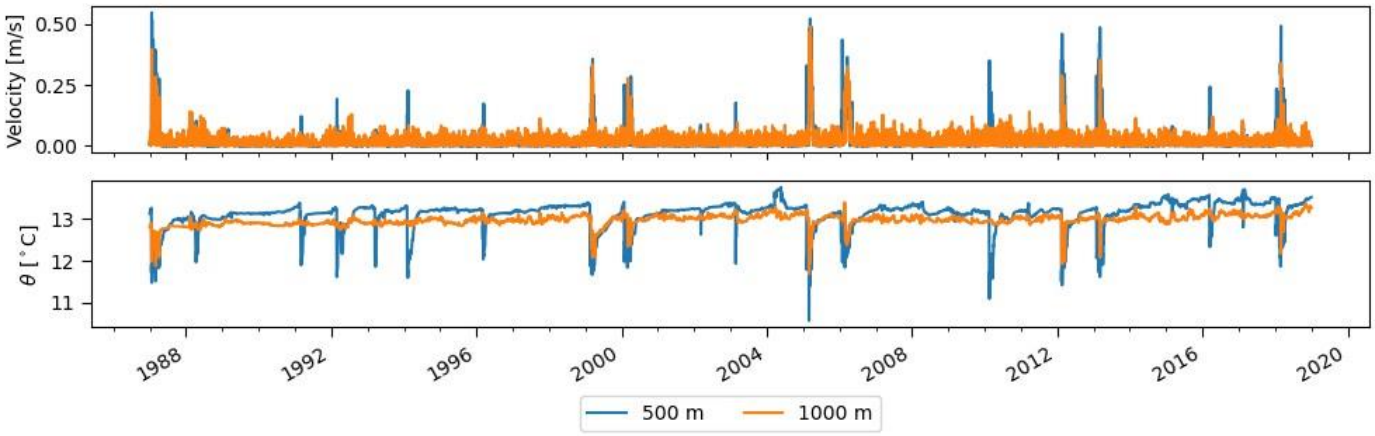

Fig 5. *Time series of the velocity and potential temperature in two locations at the bottom of the Cap de Creus Canyon.* These values correspond to the data from Med MFC.

the CCC is shown in figure 5. Cascading is evident when the time series displays an anomaly in temperature and velocity greater than -0.3ºC or +0.1 m/s respect the annual mean, at depths with no seasonal variation in temperature (> 400 m). A single anomaly at 500 m means the shelf water flow has reached at least 500 m inside the canyon: shallow cascading (level 1). If, apart from an anomaly at 500 m, an anomaly at 1000 m is depicted, shelf water will have reached more than 1000 m: deep cascading (level 2). The absence of anomalies at 500 and 1000 m means that the water has not sunk enough: no cascading (level 0). With this method, we can assign the level or intensity of cascading to each winter from 1987 to 2018. See Table I.

The anomalies at 500 and 1000 m in figure 5 perfectly match with the observations from the moorings at the canyons

Table I. Level of intensity of cascading and the associated winters from 1987 to 2018, according to Med MFC data.

	Winter
Level 0: No cascading Sinking depth < 500 m	1989, 1990, 1995, 1997, 1998, 2001, 2004, 2007, 2008, 2009, 2014, 2017
Level 1: Shallow cascading Sinking depth 500 – 1000 m	1988, 1991, 1992, 1993, 1994, 1996, 2002, 2003, 2010, 2011, 2015, 2016
Level 2: Deep cascading Sinking depth > 1000 m	1987, 1999, 2000, 2005, 2006, 2012, 2013, 2018

of LDC (500 and 1000 m) and CCC (1000 m), see the figure A.2 in the appendix section. This is another proof of the capacity of the Med MFC reanalysis to simulate continental shelf water cascading.

According to Table I and figure 5, the winters with deep cascading were: 1987, 1999, 2000, 2005, 2006, 2012, 2013, and 2018. Except for the last one, all these events have previously been reported by Bethoux et al (2002), Canals et al (2006) and Durrieu De Madron et al (2013). Notice these are paired events in two consecutive winters every 6-8 years approximately, with the first one being the most intense of the pair (lower temperature and higher cascading velocity). However, in the nineties, apart from 1999, deep cascading did not happen, according to our results. Instead, the cascading was shallow for four consecutive years (1991 to 1994), which seems unusual as it did not happen again in this 30-year long period we have analysed. Even though the shelf water was relatively cold (~11°C) (figure 4), the salinity was very low, and the density of the water did not increase enough to cascade deeper. The absence of deep cascading in that decade was also reported by Béthoux et al (2002) at LDC.

IV-2. Air-sea fluxes and river influence on density and buoyancy loss

The temperature and salinity of shelf water at the end of winter determine its maximum density, and thus, the intensity of cascading.

Ignoring the lateral advections of water with different temperature and/or salinity entering and exiting the GoL, we can analyse the interaction between the sea surface and the atmosphere, and the river influence, as sources that modify the shelf water properties. The interannual variability of this interaction should explain the interannual variability in the intensity of cascading events.

In figure 6 we have represented the net heat flux (NHF) between the ocean and the atmosphere in the shelf area of GoL, zonally and annually averaged for each winter, from December to March (DJFM). When referring to a year in winter, we mean the year of January-February-March, not the previous year in December. The Med MFC reanalysis starts in January 1987, and data of December 1986 are not available, for a DJFM mean, we need to start from winter 1988. The colours in figure 6 mean the level of intensity of cascading, as in Table I. A more negative NHF means that the sea surface of the GoL has lost more heat during a winter period. Notice that a winter with more days of strong Tramuntana wind will lead to a stronger NHF, since this wind is dry and cold, the sensible and latent heat fluxes are enhanced. The latent heat flux accounts for about 80 % of the NHF, thus, the main factor that cools the water is the evaporation.

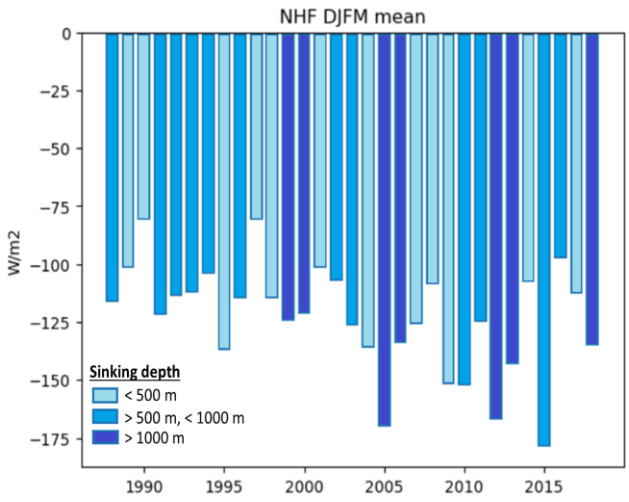

Fig 6. *Net Heat Flux (NHF) at the shelf area of the Gulf of Lion, December to March daily mean.* The negative sign means the sea loses heat towards the atmosphere. The blue tonalities correspond to the level of cascading or sinking depth of shelf water through the submarine canyon of Cap de Creus as in Table I.

According to figure 7, the three winters with a more negative NHF are 2005, 2012 and 2015. Two of these winters (2005 and 2012) are known for very intense dense shelf water cascading events at the CCC (Canals et al 2006, Durrieu De Madron et al 2012).

One would expect that the stronger the NHF in a wintertime, the colder the shelf water, and the denser, thus the deeper the sinking via cascading. Yet, the winter with stronger NHF (2015, figure 6) does not correspond to a deep cascading event (table I), whereas some winters with deep cascading (1999 and 2000) had a relatively weak NHF. Considering that NHF only accounts for thermal processes, could the mismatch between NHF and dense shelf water formation be because of changes in salinity? To evaluate this, we have plotted in figure 7 the different contributions to buoyancy loss by atmospheric and river interactions (buoyancy fluxes), including the buoyancy flux by temperature (Bt), the buoyancy flux by salinity (Bs) and the total buoyancy flux (Bs + Bt = B). Bsp represents the buoyancy flux by salinity just by precipitation-evaporation balances, without the river influence. The more negative these fluxes are, the more density the shelf water will gain, the more buoyancy it loses, the deeper the sinking.

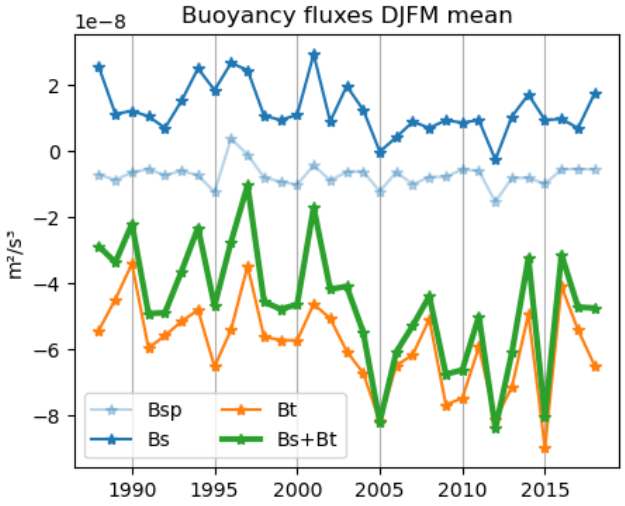

Fig 7. *Buoyancy fluxes averaged over the shelf area of the Gulf of Lion in winter.* Bs+Bt is the total buoyancy flux. Bt is the contribution by temperature changes, Bsp is by the precipitation-evaporation balance, Bs is the total contribution by salinity changes, including the river, and Bs+Bt is the total buoyancy flux.

Bs is positive because of the river discharge: the river discharge always makes the buoyancy flux more positive because it brings fresh water which is more buoyant than seawater. Bsp indicates that the precipitation-evaporation

balance is always negative: more evaporation than precipitation on average for each winter.

Bt is proportional to NHF, thus, the more negative the NHF, the more negative the Bt.

Figure 7 shows that Bt is clearly the component dominating B, because |Bs| < |Bt|. The fact that shelf water gains more density and losses buoyancy, by interaction with the atmosphere, mainly depends on the heat loss.

The winters with a less negative B (Bs+Bt) i.e., less buoyancy loss, such as 1994, 1997, 2001 (figure 7), are because Bs is more positive i.e., greater river discharge, and Bt less negative i.e., less heat loss. In these winters, Bsp is relatively less negative, which means either the precipitation was greater, or the evaporation was lesser, or both. Consequently, in 1997 and 2001 shelf water cascading did not occur. In 1994, shallow cascading occurred; seeing the T-S diagram in figure 4, we can appreciate that the shelf water was very cold but extremely fresh at the same time, thus, less dense and more buoyant.

In general, according to figure 6 and 7, the 1990s decade presents a less negative NHF and buoyancy flux than in the following decades. The cooling was milder (Bt or NHF less negative) and the freshwater input was higher (Bs more positive), mainly due to river discharge. This could explain why during that decade, apart from 1999, no deep cascading events occurred (Table I, figure 5), as previously discussed. These results are consistent with Josey et al (2011), who showed a weaker NHF on that decade over the North-Western Mediterranean.

The winters with a more negative B are 2005 and 2012, which coincide with the simulations performed by Somot et al (2018). These two winters present a very negative Bt i.e., strong heat loss, and a very low Bs, i.e., low river discharge. These were years with extremely dense shelf water, and very intense deep cascading was observed (Canals et al 2006, Durrieu De Madron et al 2013), which agrees with a more negative buoyancy flux. However, winter 2015, including the contribution by Bs, experienced a very strong buoyancy loss yet the shelf water cascading was shallow, whereas 1999 and 2000, with deep cascading events, present a relatively low buoyancy loss. The explanation for these cases may be found in the anomalies in SST in the beginning of December of the previous year: the SST in December 1998 and 1999 was unusually low (<13ºC) whereas in 2014 it was unusually high (>17.5ºC) respect the climatological mean for that time (15ºC). This affects the evaporation rates and the sensible heat fluxes because, all else being equal, a warmer water enhances evaporation (latent heat flux) and increases the contrast in temperature between the sea and the air (sensible heat flux), thus, NHF is higher in 2015. By the same reason, a lower SST at the beginning of the winter means a lower NHF, and a lower buoyancy flux for the winters 1999 and 2000. Also, a winter where SST begins warmer will require a higher energetic flux to cool this water until it reaches a high density, even if this heat flux is enhanced. This emphasises the importance of the preconditioning in dense shelf water formation.

The winters with shallow cascading present an average NHF and/or a less negative Bsp i.e., mild and/or rainy winters, for example, 1992 to 1994 and 2010.

IV-3. Modes of climate variability

The interannual variability of cascading events and buoyancy fluxes may be due to large-scale climate variability. In this region, according to Fabiano et al 2020, the three main modes of variability in winter (DJFM) are the North Atlantic Oscillation (NAO), the Atlantic Ridge (AR) and the Scandinavian Blocking (SCAN). The first three EOF patterns of the atmospheric 500hPa geopotential height variability represent these three main modes of climate variability, figure 8. Each mode oscillates in time between a positive and a negative phase, and each monthly-averaged atmospheric state is mostly explained by the combination of these three with their respective phases. A positive covariance means the geopotential height is anomalously higher, which means that the pressure at 5500m is higher than usual.

The variance fractions for NAO, AR and SCAN are 31.8%, 14.6% and 12.5%, respectively. These percentages quantify the fraction of climate variability that is due to each of the three modes.

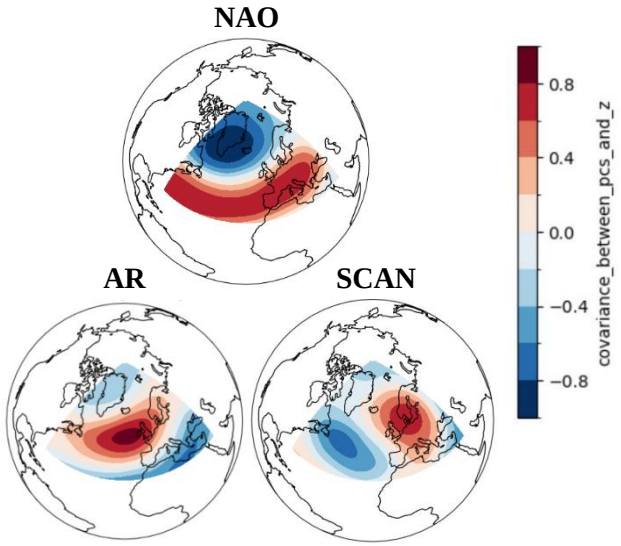

Fig 8. *Modes of climate variability represented as the covariance of the geopotential height at 500 hPa.* Red (blue) colours are positive (negative) covariances indicating positive (negative) anomalies of the geopotential height. Data from ERA5.

To examine the connection between the interannual variability of the air-sea interaction and the climate variability, we have calculated the Pearson correlation coefficients between B, Bs, Bsp, and Bt and each mode of variability in winter. The results are in Table II. Notice the negative sign of the fluxes, a positive correlation means an enhanced negative flux.

Table II. Pearson correlation coefficients between the buoyancy fluxes and the main modes of climate variability in winter (DJFM) from 1987 to 2018. Positive (negative) correlations in green (red) mean enhanced (reduced) buoyancy loss.

	-Bsp	-Bs	-Bt	-B
NAO	*0.15*	*-0.07*	-0.19	*-0.15*
AR	0.24	0.36	0.28	0.33
SCAN	-0.45	-0.16	-0.31	-0.31

Not correlated at 95% confidence interval values in grey italics.

Notice, in Table II, the correlations of Bt and B are quite similar because B is dominated by Bt.

NAO, which is the main mode that accounts for more fraction of the climate variability in this zone, is not significantly correlated with the total buoyancy flux in the GoL in winter. However, its positive phase is negatively correlated with buoyancy loss by temperature, i.e. with heat flux. This means that in winters led by a positive (negative) phase of NAO, the cooling of surface shelf water is reduced (increased).

AR is positively correlated with -Bsp, -Bs, -Bt and B. This means that the positive phase of AR mode in winter favours the buoyancy loss in the shelf zone of the GoL, by increased heat loss and decreased river discharge, and the balance precipitation-evaporation is decreased. Either the evaporation rate is higher, or the precipitation is weaker, or both.

SCAN is negatively correlated with -Bsp, -Bs, -Bt and -B, which means that when this mode has a positive phase, the buoyancy loss is reduced. In its negative phase, the negative fluxes are enhanced, since positive and negative phases have opposite effects.

These results agree with Josey et al (2011), who showed that an anomalous high pressure over the North-Atlantic, such as the AR, strengthens the heat loss in the GoL, while an anomalous high pressure over the central-northern Europe, such as SCAN, decreases the heat loss in our studied zone. The explanation for this lies on the air advection: at 500 hPa, SCAN anomalously advects air from the southeast (Mediterranean air), which is warmer and moister, whereas AR anomalously advects cold and dry air from the north (Northern Europe). This means that a winter with a positive phase of AR and negative phase of SCAN will have a colder and drier air at 500hPa. Due to the barotropic nature of these patterns, a cold advection at 500hPa may translate in a cold advection at the surface; and this increases the heat loss and buoyancy loss of shelf water at the GoL, since buoyancy loss (B) is mainly due to heat loss (Bt). This is also in accordance with Durrieu de Madron et al (2013), who claimed that AR favours strong, cold Tramuntana over the GoL.

In other words, a winter with a positive phase of AR and negative phase of SCAN is more likely to trigger dense shelf water cascading, that is the case of 2005 and 2012, but this accounts for less than 30% of the climate variability, the rest should be explained by other processes with different spatial-temporal scales like the winter preconditioning or subseasonal atmospheric variability.

V. CONCLUSIONS

This paper proves the effectiveness of the Med MFC reanalysis for the study of cascading events in the GoL. The intensity of these events represented by the model for each winter coincides with the observations, except for 2018 and 2019. The deep cascading events, when shelf water sinks below 1000 m, happen in two consecutive winters every 6-8 years; except for the nineties, where the cascading was shallow (less than 1000 m of depth) for 1991 to 1994 and 1996.

The use of reanalysis data permits a better appreciation of the whole process of the density transformation of shelf water, examine the salinity and temperature evolution and distribution of water in the GoL, and its interannual variability. The usage of different datasets for the sea, atmosphere and river, allows the comprehension of the interaction between them in the formation and sinking of dense shelf water.

Unlike open-ocean convection phenomena (Grignon et al 2010, Somot et al 2018, Margirier et al 2020), the intensity of the sinking of shelf water through the CCC does not depend on the stratification of intermediate waters (WIW, LIW), nor on the properties of LIW. It only depends on the density of the shelf water just before being funnelled down the canyon, and this is influenced by the runoff from the Rhône River. A large freshwater input from this river can disrupt the density gain of the shelf water and prevent the deep sinking of this water, as happened in 1994. This could be the explanation why in the nineties no deep cascading occurred.

Deep cascading, caused by an extremely dense shelf water, depends on the atmospheric forcing: the buoyancy loss is stronger in cold and windy winters (increased sensible and latent heat fluxes) with little precipitation and river discharge (low freshwater input), as seen in 2005 and 2012.

The formation of dense shelf water is also influenced by the pre-winter SST, i.e., preconditioning: a higher temperature at the onset of winter means that water will require more heat loss to become dense than in a winter in which the SST is cold to begin with. At the same time, a higher SST increases the energy flux between the sea and the atmosphere (more negative NHF), even though the air may not be as cold and windy as in other winters with a lower SST. Therefore, NHF averaged for a wintertime is not always indicative of a cold winter. Similarly, a stronger negative NHF does not imply that the shelf water in that year reaches a lower temperature than a winter with a weaker NHF.

In our analyses of the air-sea fluxes, we have averaged the whole shelf area for four-month-long periods, yet the huge spatial and temporal variability inside the shelf area of the GoL has not been accounted for. Lateral advections have not been analysed either, or the dense shelf water exiting the GoL southwards without funnelling to the CCC. Dense water formation and its sinking via cascading is a local phenomenon and it would be important in future studies to contemplate the residence time of the shelf water in the GoL.

Our results show that the atmospheric forcing of dense shelf water cascading is related with two modes of climate variability, AR and SCAN, whereas NAO is not significantly correlated. In the winter months with positive phases of AR and negative phases of SCAN, cold and dry air is advected over the GoL, the sea-atmosphere fluxes are intensified, the water loses more heat, gains more density, loses more buoyancy, and may end up sinking through the CCC. This fact is of great relevance because it permits to connect the winters with stronger buoyancy loss and probably deep intense cascading in the GoL with other similar phenomena in other oceans, such as the dense water formation in the Denmark Strait, provided that these phenomena are also significantly correlated with the AR and the SCAN climatic modes. This is the aim for future studies within the same project as this work, called FAR-DWO (Far-reaching impacts of dense water overflows in the North Atlantic Ocean and the Mediterranean Sea).

Acknowledgments

This TFM is part from the FAR-DWO project and Lobelia work. I want to thank Suso for all the learning I got from him; all the help, supervision, motivation and teaching I got from

Anna and David, for letting me be a part of the FAR-DWO project and participate in their cruises, and for introducing me to the company Lobelia; Víctor and Crisitan for helping and teaching me in this project, Laia for hiring me as an intern at Lobelia, Guille for MyOcean development, Ileana for supervising my report, Pere for sharing his knowledge about this topic, Josep Pascual for his data and enthusiasm, Sergi Corral for his Tramuntana studies, Ricard for helping me with programming, all the professors and classmates of the master of meteorology for all I have learned from them, and my family and friends for support. Special thanks to CEFREM and GRC-GM teams for the LDC and CCC mooring data.

VI. REFERENCES

Bergamasco, A., Sclavo, M., Carniel, S., & Schroeder, K. (2010). Dense shelf water cascading into the Cap de Creus Canyon: preliminary results from process study simulations. https://www.researchgate.net/publication/252706369

Béthoux, J. P., Durieu De Madron, X., Nyffeler, F., & Tailliez, D. (2002). Deep water in the western Mediterranean: peculiar 1999 and 2000 characteristics, shelf formation hypothesis, variability since 1970 and geochemical inferences. Journal of Marine Systems, 33(34), 117–131. https://doi.org/10.1016/S0924-7963(02)00055-6

Bryden, H. L. (1973). New polynomials for thermal expansion, adiabatic temperature gradient and potential temperature of sea water. Deep Sea Research and Oceanographic Abstracts, 20(4). https://doi.org/10.1016/0011-7471(73)90063-6

Canals, M., Puig, P., De Madron, X. D., Heussner, S., Palanques, A., & Fabres, J. (2006). Flushing submarine canyons. Nature, 444(7117), 354–357. https://doi.org/10.1038/nature05271

Company, J. B., Puig, P., Sardà, F., Palanques, A., Latasa, M., & Scharek, R. (2008). Climate influence on deep sea populations. PLoS ONE, 3(1). https://doi.org/10.1371/journal.pone.0001431

Dawson, A. (2016). eofs: A Library for EOF Analysis of Meteorological, Oceanographic, and Climate Data. Journal of Open Research Software, 4(1). https://doi.org/10.5334/jors.122

Durrieu De Madron, X., Houpert, L., Puig, P., Sanchez-Vidal, A., Testor, P., Bosse, A., Estournel, C., Somot, S., Bourrin, F., Bouin, M. N., Beauverger, M., Beguery, L., Calafat, A., Canals, M., Cassou, C., Coppola, L., Dausse, D., D'Ortenzio, F., Font, J., … Raimbault, P. (2013). Interaction of dense shelf water cascading and open-sea convection in the northwestern Mediterranean during winter 2012. Geophysical Research Letters, 40(7), 1379–1385. https://doi.org/10.1002/grl.50331

Escudier, R., Clementi, E., Omar, M., Cipollone, A., Pistoia, J., Aydogdu, A., Drudi, M., Grandi, A., Lyubartsev, V., Lecci, R., Cretí, S., Masina, S., Coppini, G., & Pinardi, N. (2020). Mediterranean Sea Physical Reanalysis (CMEMS MED-Currents) (Version 1) Data set. Copernicus Monitoring Environment Marine Service (CMEMS). https://doi.org/10.25423/CMCC/MEDSEA_MULTIYEAR_PHY_006_004_E3R1

Fabiano, F., Christensen, H. M., Strommen, K., Athanasiadis, P., Baker, A., Schiemann, R., & Corti, S. (2020). Euro-Atlantic weather Regimes in the PRIMAVERA coupled climate simulations: impact of resolution and mean state biases on model performance. Climate Dynamics, 54(11–12). https://doi.org/10.1007/s00382-020-05271-w

Fofonoff, N.P. and Millard Jr, R.C. (1983) Algorithms for the computation of fundamental properties of seawater. Paris, France, UNESCO, 53pp. (UNESCO Technical Papers in Marine Sciences; 44), https://doi.org/10.25607/OBP-1450

Grignon, L., Smeed, D. A., Bryden, H. L., & Schroeder, K. (2010). Importance of the variability of hydrographic preconditioning for deep convection in the Gulf of Lion, NW Mediterranean. Ocean Science, 6(2), 573–586. https://doi.org/10.5194/os-6-573-2010

Grimaldi, S., Salamon, P., Disperati, J., Zsoter, E., Russo, C., Ramos, A., Carton De Wiart, C., Barnard, C., Hansford, E., Gomes, G., Prudhomme, C. (2022): River discharge and related historical data from the Global Flood Awareness System. v4.0. Copernicus Climate Change Service (C3S) Climate Data Store (CDS). DOI: 10.24381/cds.a4fdd6b9

Herrmann, M., Estournel, C., Déqué, M., Marsaleix, P., Sevault, F., & Somot, S. (2008). Dense water formation in the Gulf of Lions shelf: Impact of atmospheric interannual variability and climate change. Continental Shelf Research, 28(15), 2092–2112. https://doi.org/10.1016/j.csr.2008.03.003

Hersbach, H., Bell, B., Berrisford, P., Biavati, G., Horányi, A., Muñoz Sabater, J., Nicolas, J., Peubey, C., Radu, R., Rozum, I., Schepers, D., Simmons, A., Soci, C., Dee, D., Thépaut, J-N. (2023): ERA5 hourly data on single levels from 1940 to present. Copernicus Climate Change Service (C3S) Climate Data Store (CDS), DOI: 10.24381/cds.adbb2d47 (Accessed on 22-12-2022)

Houpert, L., Durrieu de Madron, X., Testor, P., Bosse, A., D'Ortenzio, F., Bouin, M. N., Dausse, D., Le Goff, H., Kunesch, S., Labaste, M., Coppola, L., Mortier, L., & Raimbault, P. (2016). Observations of open-ocean deep convection in the northwestern Mediterranean Sea: Seasonal and interannual variability of mixing and deep water masses for the 2007-2013 Period. Journal of Geophysical Research: Oceans, 121(11), 8139–8171. https://doi.org/10.1002/2016JC011857

Josey, S. A., & Schroeder, K. (2023). Declining winter heat loss threatens continuing ocean convection at a Mediterranean dense water formation site. Environmental Research Letters, 18(2). https://doi.org/10.1088/1748-9326/aca9e4

Josey, S. A., Somot, S., & Tsimplis, M. (2011). Impacts of atmospheric modes of variability on Mediterranean Sea surface heat exchange. Journal of Geophysical Research: Oceans, 116(2). https://doi.org/10.1029/2010JC006685

Juza, M., Renault, L., Ruiz, S., & Tintoré, J. (2013). Origin and pathways of winter intermediate water in the northwestern mediterranean sea using observations and numerical simulation. Journal of Geophysical Research: Oceans, 118(12), 6621–6633. https://doi.org/10.1002/2013JC009231

Lebeaupin Brossier, C., Léger, F., Giordani, H., Beuvier, J., Bouin, M. N., Ducrocq, V., & Fourrié, N. (2017). Dense water formation in the north-western Mediterranean area during HyMeX-SOP2 in 1/36° ocean simulations: Ocean-atmosphere coupling impact. Journal of Geophysical Research: Oceans, 122(7), 5749–5773. https://doi.org/10.1002/2016JC012526

Malanotte-Rizzoli, P., Manca, B. B., Salvatore Marullo, Ribera d' Alcalá, M., Roether, W., Theocharis, A., Bergamasco, A., & Budillon, G. (2003). The Levantine Intermediate Water Experiment (LIWEX) Group: Levantine basin—A laboratory for multiple water mass formation processes. Journal of Geophysical Research, 108(C9), 8101. https://doi.org/10.1029/2002JC001643

Margirier, F., Bosse, A., Testor, P., L'Hévéder, B., Mortier, L., & Smeed, D. (2017). Characterization of Convective Plumes Associated With Oceanic Deep Convection in the Northwestern Mediterranean From High-Resolution In Situ Data Collected by Gliders. Journal of Geophysical Research: Oceans, 122(12), 9814–9826. https://doi.org/10.1002/2016JC012633

Margirier, F., Testor, P., Heslop, E., Mallil, K., Bosse, A., Houpert, L., Mortier, L., Bouin, M. N., Coppola, L., D'Ortenzio, F., Durrieu de Madron, X., Mourre, B., Prieur, L., Raimbault, P., & Taillandier, V. (2020). Abrupt warming and salinification of intermediate waters interplays with decline of deep convection in the Northwestern Mediterranean Sea. Scientific Reports, 10(1). https://doi.org/10.1038/s41598-020-77859-5

Puig, P., Madron, X. D. de, Salat, J., Schroeder, K., Martín, J., Karageorgis, A. P., Palanques, A., Roullier, F., Lopez-Jurado, J. L., Emelianov, M., Moutin, T., & Houpert, L. (2013). Thick bottom nepheloid layers in the western Mediterranean generated by deep dense shelf water cascading. Progress in Oceanography, 111. https://doi.org/10.1016/j.pocean.2012.10.003

Ribó, M., Puig, P., Palanques, A., & Lo Iacono, C. (2011). Dense shelf water cascades in the cap de creus and palamós submarine canyons during winters 2007 and 2008. Marine Geology, 284(1–4), 175–188. https://doi.org/10.1016/j.margeo.2011.04.001

Somot, S., Houpert, L., Sevault, F., Testor, P., Bosse, A., Taupier-Letage, I., Bouin, M. N., Waldman, R., Cassou, C., Sanchez-Gomez, E., Durrieu de Madron, X., Adloff, F., Nabat, P., & Herrmann, M. (2018). Characterizing, modelling and understanding the climate variability of the deep water formation in the North-Western Mediterranean Sea. Climate Dynamics, 51(3), 1179–1210. https://doi.org/10.1007/s00382-016-3295-0

Testor, P., Bosse, A., Houpert, L., Margirier, F., Mortier, L., Legoff, H., Dausse, D., Labaste, M., Karstensen, J., Hayes, D., Olita, A., Ribotti, A., Schroeder, K., Chiggiato, J., Onken, R., Heslop, E., Mourre, B., D'ortenzio, F., Mayot, N., … Conan, P. (2018). Multiscale Observations of Deep Convection in the Northwestern Mediterranean Sea During Winter 2012–2013 Using Multiple Platforms. Journal of Geophysical Research: Oceans, 123(3), 1745–1776. https://doi.org/10.1002/2016JC012671

APPENDIX

Table A.I: Constant parameters related to the fluxes between the sea and the atmosphere.

Symbol	Definition	Value	Units
ρ_a	Air referent density	1.225	Kg/m^3
L	Latent heat of vaporization	$2.466 \cdot 10^6$	J/kg
c_{pa}	Specific heat of air at constant pressure	1005	J/kg·K
C_e	Latent heat transfer coefficient	$1.4 \cdot 10^6$	None
C_h	Sensible heat transfer coefficient	10^{-3}	None
g	Gravitational acceleration	9.81	m/s^2
α_θ	Water thermal expansion coefficient	$2 \cdot 10^{-4}$	K^{-1}
ρ_s	Water referent density	1020	Kg/m^3
c_{ps}	Specific heat of water at constant pressure	4000	J/kg·K
β	Saline expansion coefficient	$7.6 \cdot 10^{-4}$	None

Table A.II: Variables related to the fluxes between the sea and the atmosphere.

Symbol	Definition	Units
q_s	Specific humidity at 98% saturation at SST (Sea Surface Temperature)	kg/kg
q_a	Specific humidity of air	kg/kg
u	Wind velocity module	m/s
T_s	Sea Surface Temperature	°C
T_a	Air temperature at 2 m	°C
SSS	Sea Surface Salinity	PSU
P	Precipitation	m/s
E	Evaporation rate = Qlatent/L· ρ_{H_2O}	m/s
R	River effect	m/s

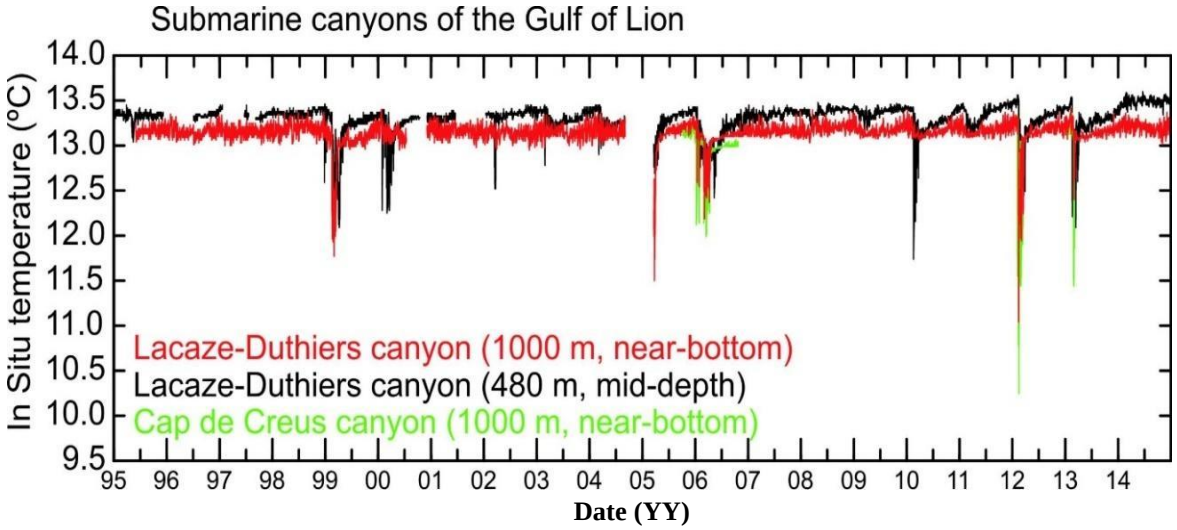

Fig A.1: *Discontinuous time series of the temperature at two depths of the Lacaze-Duthiers canyon and one at the Cap de Creus Canyon.* Data from moorings. Source: CEFREM & GRC-GM.

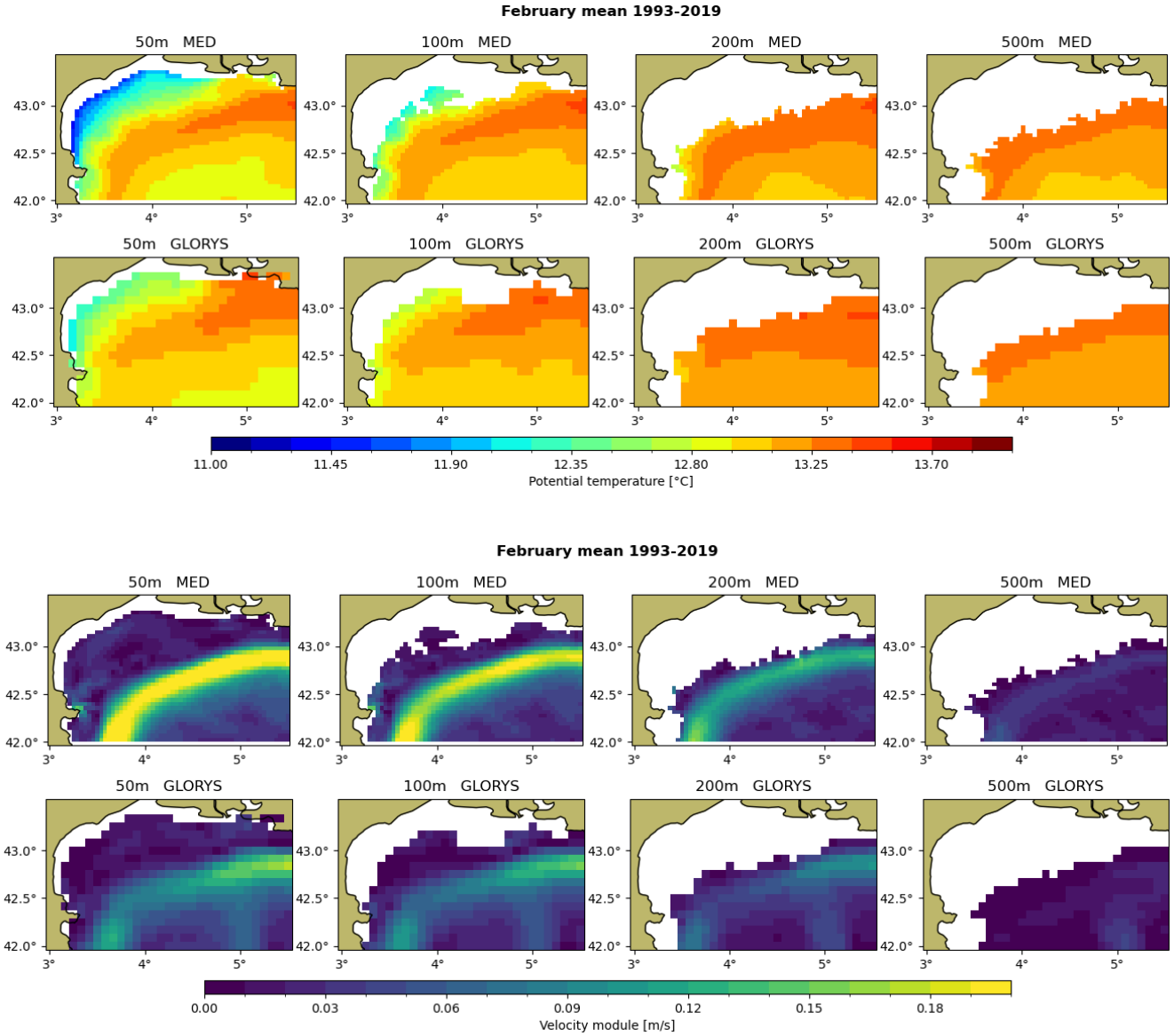

Fig A.2: *Comparison between the Med MFC (MED) and GLORYS12V1 (GLORYS) reanalyses*. The variables represented are the potential temperature (up) and the velocity of the current (down), at 50, 100, 200 and 500 meters, for the 1993-2019 February mean. Notice how the MED, with a higher resolution compared to GLORYS, represents a lower temperature at the continental shelf, and a higher velocity by the north and west sides of Cap de Creus, where the shelf water funnels down the submarine canyons. Datasets from E.U. Copernicus Marine Service Information; https://doi.org/10.48670/moi-00021, https://doi.org/10.25423/CMCC/MEDSEA_MULTIYEAR_PHY_006_004_E3R1